Feedback control of edge turbulence in a tokamak

Zhai Kan,[1,2] Wen Yi-zhi,[1] Yu Chang-xuan,[1] Liu Wan-dong,[1] Wang Chao,[1] Zhuang Ge,[1] and Xu Zhi-zhan[2]
[1]*Department of Modern Physics, University of Science and Technology of China, Hefei, Anhui, 230027, China*
[2]*Shanghai Institute of Optics and Fine Mechanics, Academia Sinica, 201800, Shanghai, China*
(Received 11 June 1996)

An experiment on feedback control of edge turbulence has been undertaken on the KT-5C tokamak. The results indicate that the edge turbulence could be suppressed or enhanced depending on the phase shift of the feedback network. In a typical case of 90° phase shift feedback, the turbulence amplitudes of both $\tilde{T}_e$ and $\tilde{n}_e$ were reduced by about 25% when the gain of the feedback network was 15. Correspondingly the radial particle flux decreased to about 75% level of the background. Through bispectral analysis it is found that there exists a substantial nonlinear coupling between various modes comprised in edge turbulence, especially in the frequency range from about 10 kHz to 100 kHz, which contains the large part of the edge turbulence energy in *KT*-5*C* tokamak. In particular, by actively controlling the turbulence amplitude using feedback, a direct experimental evidence of the link between the nonlinear wave-wave coupling over the whole spectrum in turbulence, the saturated turbulence amplitude, and the radial particle flux was provided. [S1063-651X(97)05703-6]

PACS number(s): 52.75.−d, 52.35.Mw, 52.35.Ra

I. INTRODUCTION

A major roadblock to plasma confinement in a tokamak is due to anomalous transport, which cannot be described by the present neoclassical theories of simple Coulomb collisions of electrons and ions orbiting in the sheared magnetic field [1–3]. Generally plasma turbulence has been considered as a probable source of the anomalous heat and particle transport in tokamaks. Experiments have shown that transport due to turbulent electrostatic fluctuations can account for most of the edge plasma particle and heat transport [4–6]. Moreover, many theoretical models of plasma edge fluctuations also indicate a strongly turbulent nature with significant consequences for transport [7–9]. Not only from the highly turbulent edge region serving as a boundary for the interior plasma but also from the experimental observations of improved plasma confinement in tokamaks [10,11], it is suggested that edge confinement plays a critical role in the determination of a global plasma confinement. Therefore, a main task in magnetic confinement plasma physics is to find a way to actively control the edge turbulence. Early work shows the feasibility of suppressing plasma instabilities using feedback control techniques, for example, the feedback experiments to suppress the drift instability in hollow-cathode arc discharge plasma [12], the flute instability in the plasma produced by a Lisitano type electron-cyclotron resonance heating structure [13], and, particularly, a series of experiments carried out successfully on the Columbia Linear Machine [14–17]. These experiments not only serve as excellent paradigms but also resolve the basic physics issues for control of tokamak instabilities [14]. However, all these experiments involve only one single mode or two modes with a well-defined frequency and wave number. But in a tokamak edge the turbulence is generated through the strong nonlinear coupling of various modes and is manifested with a broadband spectrum characterized by short perpendicular wavelengths and short perpendicular correlation lengths [1–3]. Therefore, the previous feedback work cannot be directly applicable to the plasma edge turbulence in tokamaks. However, the experiment carried out on the Texas Experimental Tokamak (TEXT) indicates that edge turbulence can be enhanced or reduced by applying feedback [18–21], and that the effects of feedback depend upon the phase shift and the gain of the feedback network.

In this paper the experimental results on feedback control of the edge turbulence on KT-5C are presented. In particular, by using this feedback control technique we can actively control the edge turbulence amplitude to provide direct experimental evidence of the connection between the nonlinear coupling of the various modes comprised in turbulence, the turbulence amplitude, and the radial particle flux. All these could not only provide substantial experimental information on the investigations in new applications of effective control of edge turbulence to achieve an improved plasma confinement but also help to understand the properties and the origin of the turbulence. This paper is organized in the following way. In Sec. II, we describe the experimental setup and the details of the data analysis techniques. The experimental results and discussion on the feedback effects are presented in Sec. III. A summary and conclusions of this work are contained in Sec. IV.

II. EXPERIMENTAL SETUP AND ANALYSIS TECHNIQUES

The KT-5C tokamak is a small size, ohmically heated tokamak with the following parameters, major radius $R=32.5$ cm, plasma radius $a=9.5$ cm, plasma current $I_p=10\sim20$ kA, toroidal field $B_t\leqslant0.7$ T, electron density $n_e=10^{18}\sim10^{19}$ m^{-3}, plasma duration time $\tau_p\approx2$ ms, central electron temperature $T_e\approx100$ ev.

Figure 1 depicts the schematic diagram of the experimental setup. Two sets of movable Langmuir probes have been used in the experiment, which have identical geometrical configurations and dimensions, as shown in Fig. 1. Each probe pin is made of a tungsten rod with 1 mm diameter and

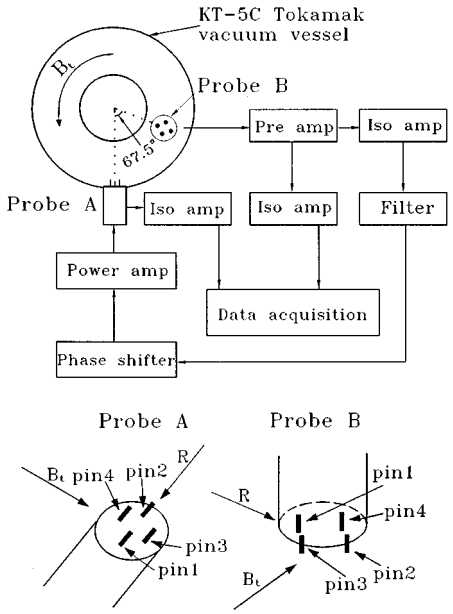

FIG. 1. Schematic diagram of the experimental setup, showing the construction of the probes and their orientation to KT-5C tokamak.

the tip length is 2 mm. The center distance of the adjacent two pins is 5 mm. A power amplifier with a frequency bandwidth from 1 kHz to 200 kHz and a 3.5 kW peak output power is used to drive the two pins ($A1$ and $A2$) on one probe called probe A. The driving current is sampled through an inductionless resistor of 0.6 Ω. Another probe called probe B is used to measure the floating potential as the feedback signal through a constant phase shifter after being preamplified and filtered. The relative position of these two probes is shown in Fig. 1, with probe A placed in the horizontal direction and probe B in the vertical direction separated 67.5° toroidally from probe A. The power amplifier is utilized with its ground floating, while the experimental setup on TEXT with its power amplifier working with a dc bias [18–21]. A 16-channel and 12-bit digitizer is used to record experiment data at the sample rate of 500 kHz. Since most energy of the edge turbulence is generally concentrated in the frequency range from 10 kHz to 200 kHz, a butterworth high-pass filter with $n=2$ is utilized to filter the dc and low frequency components. This filter would introduce an additional phase shift which we will mention later. According to the principles of the control science [22], the phase shift and gain are the key issues of a feedback network. A constant 90° phase shifter is used in our experiment. We thus have four options for the phase shift of the feedback network, that is, 0°,90°,180°, and −90°, by switching the power amplifier to work in a state of in-phase or out-of-phase.

In our experiment the KT-5C tokamak is operated with its toroidal field B_t and plasma current I_p in a typical case, in which probe A and probe B are placed on the same magnetic field line. This magnetic field line rotates helically about a 5/4 circle along the toroidal direction and about a 1/4 circle in the poloidal direction, connecting probe A and probe B. Probe A and probe B are inserted at $r=9$ cm, just 0.5 cm inside the full circular limiter, in order to keep the magnetic connection between these two probes. Along the magnetic field line the distance from probe A to probe B is approximately 3 m. Besides the detailed calculations of the magnetics of KT-5C, a wave-launching system is used in our experiment to ensure the configurations that probe A and probe B are located on the same magnetic field line. Earlier experiments on the KT-5C [23] and the TEXT [18–20] indicate that the propagation of the externally excited fluctuation is taking place along the magnetic field line. This result could be used to calibrate the required configuration in our experiment. Applying a signal of 50 kHz from a function generator and then being power amplified on pin $A1$ and $A2$, there would appear a peak at the driving frequency in the power spectrum of the floating potential fluctuation measured by probe B by adjusting the toroidal field B_t and plasma current I_p to appropriate values. Fine tuning B_t and I_p, the peak in the power spectrum can reach a maximum, which means that probe A and probe B are located on the same magnetic field line. This phenomenon itself demonstrates that the stationary plasma discharge required by the experimental configuration is well satisfied. Besides, no apparent change of the flat top of the plasma current recorded by the digitizer (12-bit, linear precision better than 0.1%) has been observed between separate discharges. All these facts indicate that the required configuration is well established on KT-5C.

The standard spectral analysis technique is used to process data [24–27]. For a measured signal $\phi(x,t)$ consisting of N samples $\phi(x,l\Delta t)$ where $l=0,\ldots,N-1$, the sample interval $\Delta t=T/N$, the record time T, the sample discrete Fourier series coefficient may be computed,

$$\tilde{\Phi}(x,f)=\frac{1}{N}\sum_{l=0}^{N-1}\phi(x,l\Delta t)\exp(-i2\pi fl\Delta t), \tag{1}$$

where $f=n\Delta f$ in which $n=0,\ldots,N-1$, and $\Delta f=T^{-1}$ is the frequency resolution. The autopower spectrum is given by

$$P(x,f)=\tilde{\Phi}^{*}(x,f)\tilde{\Phi}(x,f). \tag{2}$$

For the given signals $\phi_1(x_1,l\Delta t)$ and $\phi_2(x_2,l\Delta t)$, their discrete Fourier series coefficients are $\tilde{\Phi}_1(x_1,f)$ and $\tilde{\Phi}_2(x_2,f)$, then the sample cross spectrum is

$$P_{\phi_1\phi_2}(f)=\tilde{\Phi}_1^{*}(x_1,f)\tilde{\Phi}_2(x_2,f)=C(f)+iQ(f), \tag{3}$$

where $C(f)$ and $Q(f)$ are, respectively, the in-phase and quadrature components of the cross spectrum. The phase angle between ϕ_1 and ϕ_2 is

$$\theta_{\phi_1\phi_2}(f)=\tan^{-1}[Q(f)/C(f)]. \tag{4}$$

If ϕ_1 and ϕ_2 are the same physics parameters measured at two different locations, the sample local wave number is then given by

$$k(f)=\theta_{\phi_1\phi_2}(f)/x_p, \tag{5}$$

where $x_p = x_1 - x_2$ is the distance between the location of the two measured signals.

In order to acquire the ensemble average to reduce the statistical error level, every value we used in the spectral analysis is the average value over 30 or 60 successive shots. The data we used are acquired at the time corresponding to the flat part of the plasma current.

III. EXPERIMENTAL RESULTS AND DISCUSSION

A. Feedback control results

When direct feedback is applied, the power spectrum of the floating potential fluctuation measured by pin $A3$ is displayed in Fig. 2(a). It is shown that the turbulence was enhanced in the spectrum below 100 kHz. This enhancement is not only localized at the location of probe A, but the turbulence measured by pin $B1$ also shows this enhancement, as in Fig. 2(b). Through correlation analysis between the input and output of the feedback network, the phase shift of the feedback network can be derived, as shown in Fig. 2(c). It can be seen in this figure that the phase shift is almost 0° in the range of 30 kHz to 150 kHz. At a frequency below 30 kHz there exists an apparent phase shift; this may be attributed to the use of the high-pass filter which can introduce an additional phase shift at low frequency. As to the additional phase shift above 150 kHz, it may be due to the frequency response of the feedback network not being high enough to respond to the variation with a frequency exceeding 150 kHz.

Similar results can be obtained when feedback with a 180° phase shift was applied, the turbulence amplitude becomes greater than it is without feedback, as shown in Fig. 3. However, there exists a difference when a $-90°$ phase shift feedback is applied. It is obvious that besides the turbulence being enhanced in the frequency range below 100 kHz, as above, there appears a sharp peak in the power spectrum of the measured floating potential fluctuation, which is shown in Fig. 4.

A typical case which shows encouraging results is the feedback with a 90° phase shift. The power spectrum of the floating potential fluctuation measured by pin $A3$ under such a feedback is shown in Fig. 5(a). It is obvious that the whole spectrum below about 100 kHz were reduced to about the 75% level as the background. Figure 5(b) displays the phase angle between the input and output of the feedback network, which denotes the phase shift of this feedback network.

We repeat the above experiments with the difference that the feedback signal comes from the measurement of pin $A3$, which is the analog of the near sensor feedback on the TEXT [18–21]. From these experiments the same results have been obtained as above, which are as follows: (1) when a $0°, 180°$, or $-90°$ phase shift feedback is applied, the turbulence amplitude is enhanced; (2) when a 90° phase shift feedback is applied, the turbulence is reduced; (3) the feedback effects, with enhanced or reduced turbulence amplitude, are not localized at the location of probe A but are also at the location of probe B. It is also found that when the toroidal field B_t or the plasma current I_p is changed, probe A and probe B cannot be maintained on the same field line, the feedback effects vanishes in the measurement of pin $B1$, no matter whether that the feedback signal comes from pin $A3$ or pin $B1$. These facts indicate that the extent of the feedback effects are limited along the magnetic field line. However, our feedback experimental results differ from those on the TEXT [18,19], where the turbulence is reduced with an out-of-phase feedback and enhanced with an in-phase feedback. This may be due to the difference in the arrangement of the feedback network and the parameters of the plasma in these two devices.

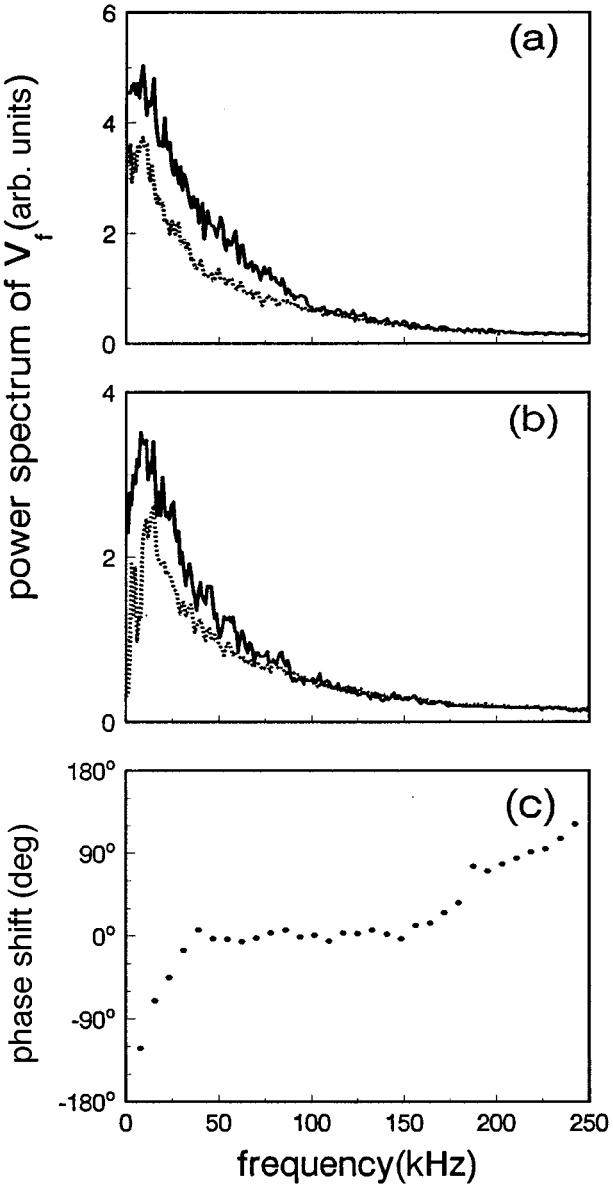

FIG. 2. Power spectrum of the floating potential fluctuation measured by (a) pin $A3$ and (b) pin $B1$. The dotted line indicates the background case and the solid line corresponds to the case under direct feedback with a gain of 15. (c) Phase shift of the feedback network obtained through the correlation analysis between the input and output of the feedback network.

The above experiments have been done by fixing the gain of the feedback network to be 15. We also have undertaken the experiments with a different gain of the feedback network. The results indicate that the higher the gain of the feedback network, the more effective the feedback appears. Figure 6 shows the power spectrum of the floating potential

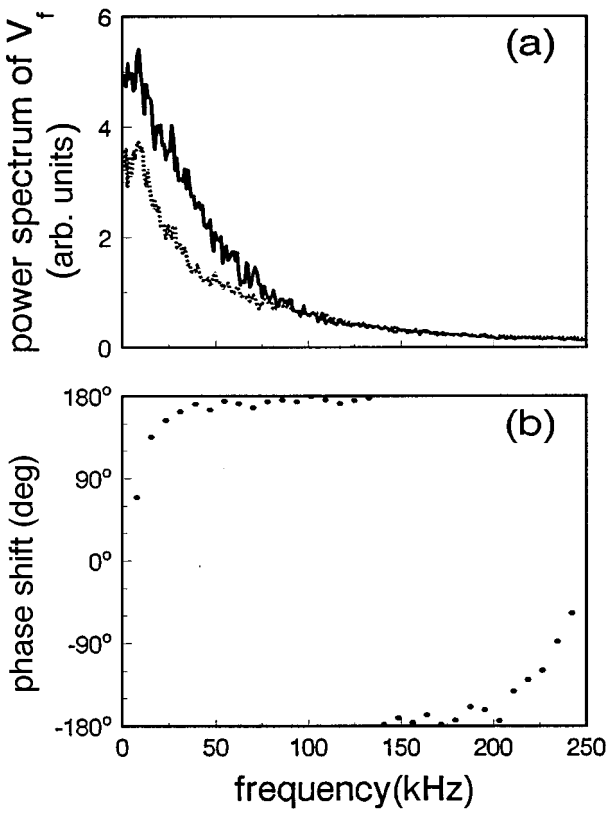

FIG. 3. (a) Power spectrum of the floating potential fluctuation measured by pin $A3$. The dotted line indicates the background turbulence and the solid line indicates the result by applying a feedback with a phase shift of 180° and a gain of 15. (b) Phase shift of the feedback network.

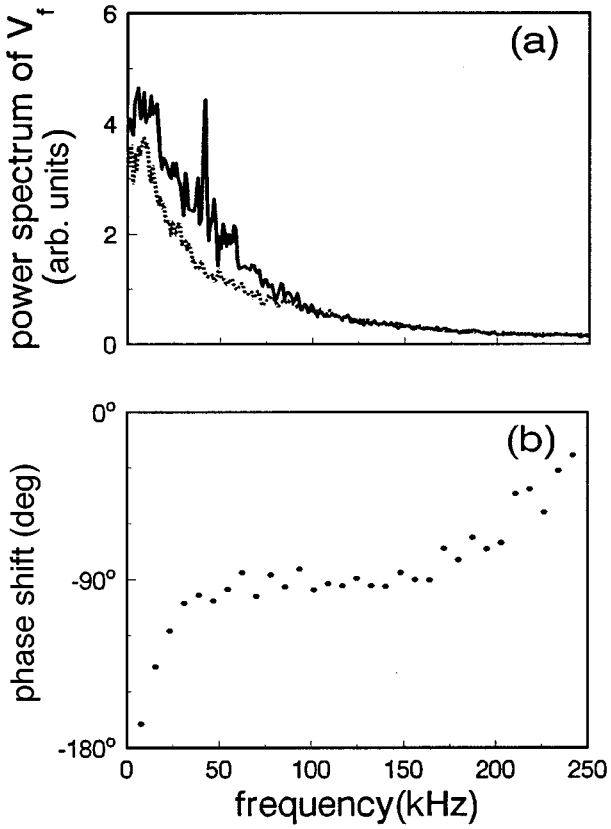

FIG. 4. (a) Power spectrum of the floating potential fluctuation measured by pin $A3$. The dotted line indicates the background turbulence and the solid line indicates the result by applying a feedback with a phase shift of $-90°$ and a gain of 15. (b) Phase shift of the feedback network.

fluctuation measured by pin $A3$ in the feedback with a phase shift of 0° and 90° and a gain of 10 and 15, respectively, in the case where the feedback signal is derived from the measurement of pin $B1$.

From the above experiments, it is found that the feedback effects are mainly dependent upon the phase shift and the gain of the feedback network, regardless of the location from which the feedback signal comes; this is in agreement with the result on TEXT [18,19]. The reason for this could be the high correlation of the edge turbulence along the magnetic field line and the long parallel wavelength of the highly correlated edge turbulence. However, these edge turbulence properties have been studied extensively in previous experiments [4,27–30].

The effects of feedback on the fluctuating electron density, as well as the fluctuating electron temperature, are also investigated in our experiment. According to the triple-probe theory [31], applying an external constant voltage V_0 ($V_0 \geqslant 4T_e$, to ensure the collection of ion saturation current) between pin $B3$ and $B4$, while making pins $B1$ and $B2$ float in plasma to measure the floating potential at their locations; thus, the fluctuation of the electron temperature can be directly derived by

$$\tilde{T}_e(t) = (\ln 2)^{-1} \tilde{V}_d, \tag{6}$$

in which V_d is the potential difference between the floating potential and the potential of the positively biased probe pin.

The electron density fluctuation can be derived through the measurement of the ion saturation current,

$$\tilde{n}_e(t) = \frac{\alpha \tilde{I}_{ion}}{\sqrt{T_e}}. \tag{7}$$

Results similar to those of the potential fluctuation have been observed for the fluctuating electron density and electron temperature at different feedback arrangements. In order to get a clear comparison between the feedback results and the background, we calculated the fluctuation amplitude in different feedback arrangements through the probe measurement. The root-mean-square value of the fluctuation amplitude is defined as

$$\tilde{n}_e = \langle [\langle \tilde{n}_e(t) \rangle - \tilde{n}_e(t)]^2 \rangle^{1/2}, \tag{8}$$

$$\tilde{T}_e = \langle [\langle \tilde{T}_e(t) \rangle - \tilde{T}_e(t)]^2 \rangle^{1/2}. \tag{9}$$

Here $\langle\ \rangle$ denote the time average, instead of the ensemble average when the time is long enough. Table I and Table II give the normalized fluctuation level of $\tilde{n}_e$ and $\tilde{T}_e$ measured by probe B in different feedback arrangements, including their background values. It is shown in Table I and Table II that the fluctuation amplitudes of both $\tilde{T}_e$ and $\tilde{n}_e$ are increased in the feedback with a phase shift of

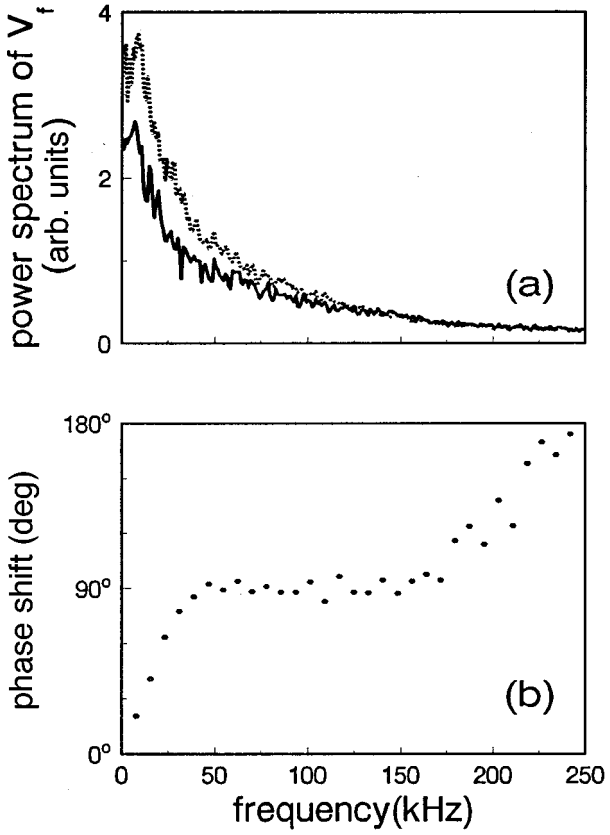

FIG. 5. (a) Power spectrum of the floating potential fluctuation measured by pin $A3$. The dotted line indicates the background turbulence and the solid line indicates the result by applying a feedback with a phase shift of 90° and a gain of 15. (b) Phase shift of the feedback network.

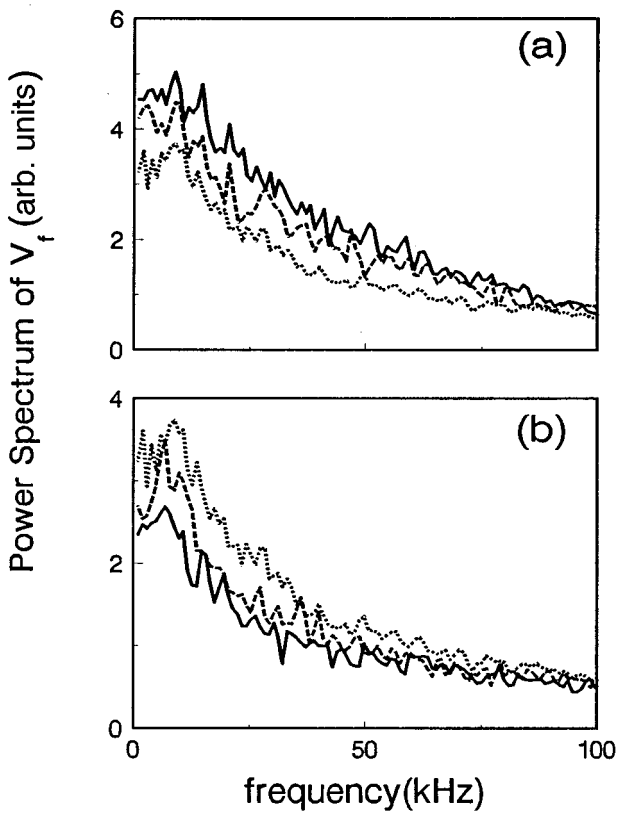

FIG. 6. Power spectrum of the floating potential fluctuation measured by pin $A3$ under different feedback arrangements; the dotted line indicates the background turbulence, the dashed line indicates the case with a gain of 10, and the solid line indicates the case with a gain of 15. (a) Direct feedback and (b) feedback with 90° phase shift.

$0°, 180°, -90°$. On the other hand, they are decreased in the 90° phase shift feedback. This can be taken as the cross-check of the above spectrum analysis in different feedback arrangements.

A coupling between the plasma density and radial velocity fluctuation can give rise to a radial particle flux [25,27]. This electrostatic fluctuation-driven particle flux can be determined from a cross-correlation analysis between the fluctuation of plasma density and the poloidal electric field. By averaging the cross correlation over time instead of an ensemble average, we obtain a steady-state fluctuation-driven particle flux across the magnetic field,

$$\Gamma_\perp = \langle \tilde{n}\tilde{v}_\perp \rangle = \frac{4\pi}{B}\int_0^\infty k_\theta(f)|P_{n\phi}(f)|\sin[\theta_{n\phi}(f)]df, \tag{10}$$

where k_θ is the local wave number determined by the cross correlation of the floating potential fluctuation measured by two poloidally placed probe pins, $B1$ and $B2$. $P_{n\phi}$ and $\theta_{n\phi}$ are the cross spectrum and phase angle between the density and potential fluctuations, respectively. In principle, this technique requires that the probe pin separation must be small enough so that all the probe pins are located within the high correlation column, and π/x_p (x_p is the separation of two poloidally placed probe pins) is greater than the highest wave number of any significant spectral component to avoid indeterminacies of $\pm n2\pi/x_p$ in the measured wave number. However, edge turbulence measurements from diverse machines exhibit a general consistency, for example, the average poloidal wave number $\bar{k}_\theta$ lies in the range of $2-4\,\mathrm{cm}^{-1}$ and the poloidal correlation length is about $1-2$ cm [1–3,27–30]. This ensures that our probe design is appropriate for estimating the particle flux. In addition, the successful application of a similar probe (0.45 cm separation between adjacent probes) on a similar tokamak (Pretext) suggests the validity of our analysis of the data obtained from the probe measurement [27]. Furthermore, we have compared the flux via this spectral analysis technique with the flux calculated from the data obtained by the sweeping double probe with a smaller probe separation of 3 mm [32].

TABLE I. Normalized electron density fluctuation $\tilde{n}_e/n_e$ in different feedback arrangements, the background value is 0.72. n_e is the equilibrium electron density at the location of probe B.

Phase shift	Gain=10	Gain=15
0°	0.82	0.87
90°	0.61	0.54
180°	0.79	0.84
−90°	0.93	1.03

TABLE II. Normalized electron temperature fluctuation $\tilde{T}_e/T_e$ in different feedback arrangements, the background value is 0.37. T_e is the equilibrium electron temperature at the location of probe B.

Phase shift	Gain=10	Gain=15
0°	0.43	0.44
90°	0.32	0.29
180°	0.41	0.46
−90°	0.47	0.51

There was agreement within experimental error for these two independent techniques. These facts serve as a strong indication that the analysis and the application of such techniques in our experiment are being correctly performed and that the plasma phenomena being investigated are accurately characterized. Table III presents the radial particle flux $\Gamma_\perp$ measured by probe B in different feedback arrangements, including its background values. It is shown in this table that corresponding to the increase (or decrease) of the fluctuations amplitude the radial particle flux also increases (or decreases). This one to one connection, to some extent, could be considered as the analogy that improved confinement can be achieved when the edge fluctuations are reduced due to the sheared poloidal rotation in the transition from L mode to H mode confinement.

B. Nonlinear nature of the edge turbulence

Most models of plasma turbulence predict that the instabilities are saturated through wave-wave interactions transferring the fluctuation energy to wave-number-frequency components that dissipate the energy [33,34]. A bispectral analysis could provide the information about the nonlinear interaction of wave-wave coupling in turbulence [35,36]. The bicoherency of the signal $\phi(t)$ is defined as

$$b^2(f_1,f_2)=\frac{\langle\tilde{\Phi}(f_1)\tilde{\Phi}(f_2)\tilde{\Phi}^*(f)\rangle^2}{[\langle|\tilde{\Phi}(f_1)\tilde{\Phi}(f_2)|^2\rangle P(f)]}, \tag{11}$$

where $P(f)$ is the autopower spectrum of ϕ and $\tilde{\Phi}(f)$ is the Fourier transform of the time trace $\phi(t)$. The bicoherency measures the fraction of the fluctuation power at a frequency f, which is phase correlated with the spectral components at frequency f_1 and f_2 obeying the summation rule $f=f_1\pm f_2$. Physically the bicoherency will take on a value close to unity when the wave at $f=f_1\pm f_2$ is excited by coupling of the waves at f_1 and f_2. On the other hand, a value of $b^2(f_1,f_2)$ near zero implies an absence of coherence for the interaction and, thus, suggests that the waves at f_1,f_2 and $f=f_1\pm f_2$ may be spontaneously excited independent modes of a system. For the purpose of this paper it is sufficient to present the integrated bicoherency

$$b^2(f)=\sum_{f_1\pm f_2=f} b^2(f_1,f_2), \tag{12}$$

which represents the fraction of the total power at f which is coupled through three-wave interactions. It allows one to discriminate between waves spontaneously excited in plasma and those generated by the former through nonlinear coupling.

TABLE III. The radial particle flux $\Gamma_\perp$ measured by probe B in different feedback arrangement, the background value is 1.13 (10^{16}/cm^2 s).

Phase shift	Gain=10	Gain=15
0°	1.21	1.28
90°	0.93	0.87
180°	1.23	1.31
−90°	1.32	1.49

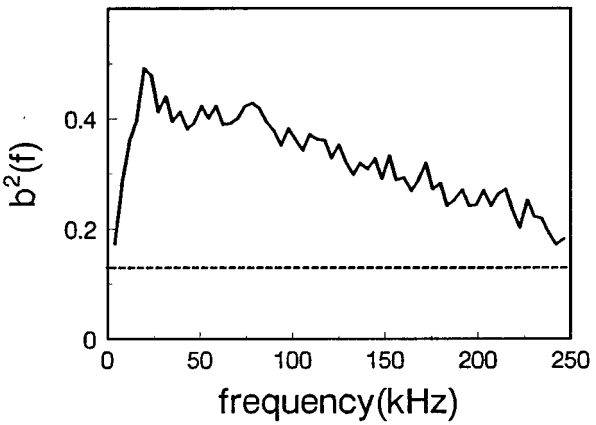

FIG. 7. The integrated bicoherency $b^2(f)$ of the background floating potential fluctuation measured by pin $A3$. Dashed line indicates the experimental uncertainty $\gamma=0.13$.

Figure 7 displays the integrated bicoherency $b^2(f)$ of the background fluctuation of the floating potential measured by pin $A3$, the dotted line indicates the experimental uncertainty $\gamma(\gamma=\Sigma_{f_1\pm f_2=f}1/M\approx 0.13$ where M is the number of realizations). It is shown that the obtained $b^2(f)$, in the whole spectrum, is large compared to γ, which means that there does exist nonlinear interactions between the various modes in turbulence. It is clear, in this figure, that the degree of the nonlinear coupling decreases while the frequency increases. Since the turbulence energy is mainly concentrated in the frequency range of 10 kHz to 100 kHz in the KT-5C tokamak, as shown in Fig. 2, it is suggested that part of this energy comes from the redistribution of the energy contained in plasma instabilities through the nonlinear mode coupling.

The $b^2(f)$ from the measurement of pin $A3$, in different feedback arrangements, are plotted in Fig. 8. For comparison the background $b^2(f)$ is also given in each subfigure. The $b^2(f)$ spectra, in different feedback, show the same tendency as the background $b^2(f)$, with the role of nonlinear coupling decreasing as the frequency increases. However, the main feature of these plots is the variation of the degree of the nonlinear interaction in the whole spectrum. Under positive feedback, which indicates the case that the turbulence is enhanced, the strength of $b^2(f)$ is reduced, as shown in Figs. 8(a), 8(c), and 8(d). On the contrary, while in negative feedback the strength of $b^2(f)$ is increased, as shown in Fig. 8(b). This result demonstrates that there exists an interlink

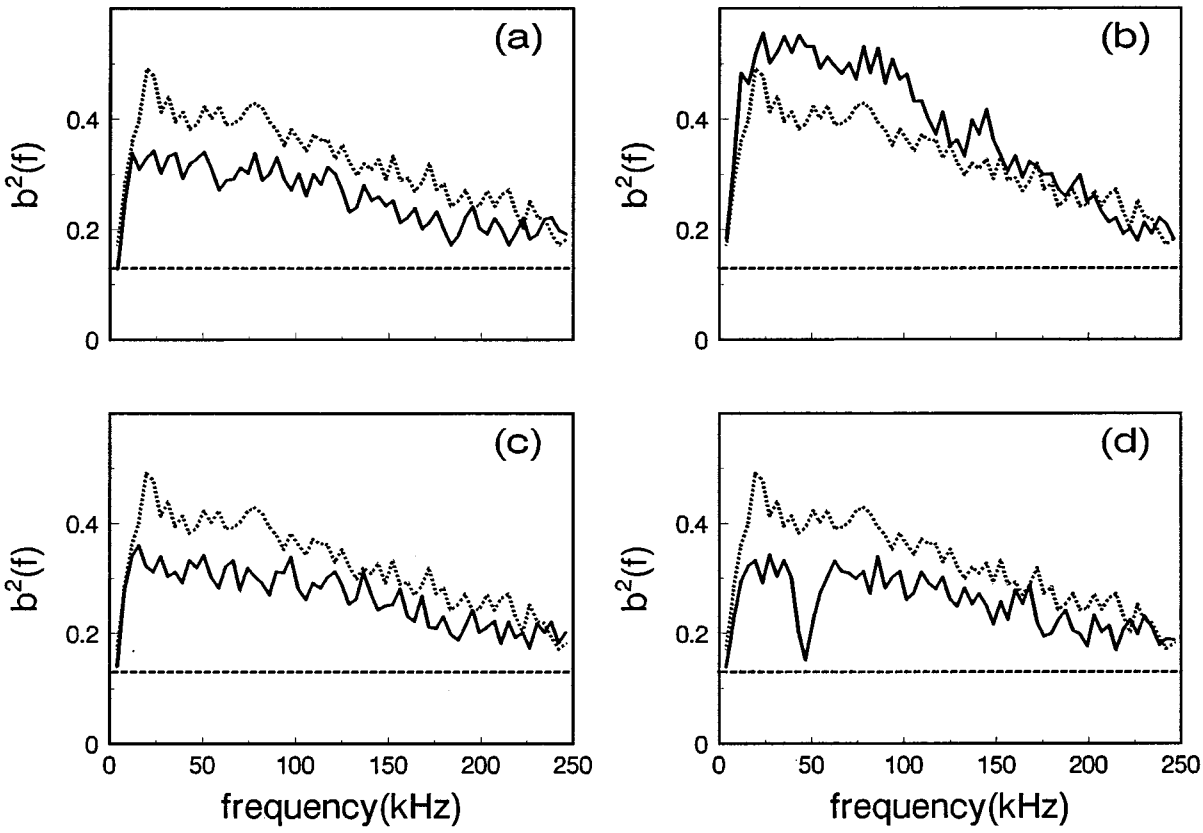

FIG. 8. The integrated bicoherency $b^2(f)$ of the floating potential fluctuation measured by pin $A3$ in different feedback arrangement, (a) direct feedback, (b) feedback with 90° phase shift, (c) feedback with 180° phase shift, and (d) feedback with $-90°$ phase shift. The dotted line indicates the background, the solid line indicates the feedback results, and the dashed line indicates the experimental uncertainty $\gamma = 0.13$.

between the nonlinear wave-wave interaction of the various modes in turbulence, the turbulence saturated amplitude, and the radial particle flux. When the degree of nonlinear interaction increases, the turbulence saturated amplitude decreases, and, thus, the radial particle flux decreases. On the other hand, when the role of the nonlinear interaction decreases, the saturated turbulence amplitude increases and the radial particle flux increases correspondingly. The minimum in the $b^2(f)$ plot in the case with $-90°$ phase shift feedback in Fig. 8(d) means that the peak in the power spectrum in Fig. 4(a) corresponds to an almost spontaneously excited mode, and is not generated by the nonlinear mode coupling.

IV. SUMMARY

The experiment in actively controlling edge turbulence through feedback techniques has been carried out on the KT-5C tokamak by using two Langmuir probe sets. The results indicate that the effect of the feedback is mainly determined by the phase shift and the gain of the feedback network, having little dependence at all upon the location where the feedback signal was obtained. Under different feedback arrangements, the turbulence along the magnetic field line can be enhanced or reduced. The tendency to enhance or reduce the turbulence is determined by the phase shift of the feedback network. On the other hand, the factor for the enhancement or reduction of the turbulence is determined by the gain of the feedback network. In the particular case of 90° phase shift feedback, the amplitude of floating potential fluctuation spectrum components, the absolute fluctuation levels of both $\tilde{T}_e$ and $\tilde{n}_e$ were reduced by about 25% when the gain of the feedback network is 15. Correspondingly, the radial particle flux decreased to about 75% of the background level. Through bispectral analysis, it is found that there does exist the nonlinear wave-wave couplings between the various modes in turbulence, which might redistribute the energy contained in plasma instabilities and concentrate the energy in the low frequency from about 10 kHz to 100 kHz. Furthermore, by actively controlling the turbulence amplitude, a direct experimental evidence of the connection between the strength of the nonlinear interaction, the saturated turbulence amplitude, and the radial particle flux was provided. All these results obtained in our experiment could provide important benchmarks for a better understanding of the plasma turbulence nature and make a significant contribution to the discovery of new applications to control the edge turbulence to achieve improved plasma confinement.

ACKNOWLEDGMENT

Helpful discussions with Dr. G. D. Wang, Dr. C. Wang, and Dr. Y. H. Xu are gratefully acknowledged. The authors would like to thank the KT-5C staff for their support in this experiment. This work was supported by the Chinese Academy of Science and High-Tech Project of China.

[1] A. J. Wootton, B. A. Carreras, H. Matsumoto, K. McGuire, W. A. Peebles, Ch. P. Ritz, P. W. Terry, and S. J. Zweben, Phys. Fluids B **2**, 2879 (1990).
[2] P. C. Liewer, Nucl. Fusion **25**, 543 (1985).
[3] J. D. Callen, Phys. Fluids B **4**, 2142 (1992).
[4] Ch. P. Ritz, R. D. Bengtson, S. J. Levinson, and E. J. Powers, Phys. Fluids **27**, 2956 (1984).
[5] Ch. P. Ritz, R. V. Bravenec, P. M. Schoch, R. D. Bengtson, J. A. Boedo, J. C. Forster, K. W. Gentle, Y. He, R. L. Hickok, Y. J. Kim, H. Lin, P. E. Phillips, T. L. Rhodes, W. L. Rowan, P. M. Valanju, and A. J. Wootton, Phys. Rev. Lett. **62**, 1844 (1989).
[6] P. C. Liewer, J. M. McChesney, S. J. Zweben, and R. W. Gould, Phys. Fluids **29**, 309 (1986).
[7] P. W. Terry and P. H. Diamond, Phys. Fluids **28**, 1419 (1985).
[8] T. S. Hahm, P. H. Diamond, P. W. Terry, L. Garcia, and B. A. Carreras, Phys. Fluids **30**, 1452 (1987).
[9] L. Garcia, P. H. Diamond, B. A. Carreras, and J. D. Callen, Phys. Fluids **28**, 2147 (1985).
[10] F. Wagner *et al.*, Phys. Rev. Lett. **49**, 1408 (1982).
[11] R. J. Taylor, M. L. Brown, B. D. Fried, H. Grote, J. R. Liberati, G. J. Morales, P. Pribyl, D. Darrow, and M. Ono, Phys. Rev. Lett. **63**, 2365 (1989).
[12] B. E. Keen and R. V. Aldridge, Phys. Rev. Lett. **22**, 1358 (1969).
[13] R. K. Richards, G. A. Emmert, and D. P. Grubb, Plasma Phys. **17**, 271 (1975).
[14] A. K. Sen, Phys. Plasmas **1**, 1479 (1994).
[15] P. Tham and A. K. Sen, Phys. Fluids B **4**, 3058 (1992).
[16] P. Tham and A. K. Sen, Phys. Rev. A **46**, R4520 (1992).
[17] P. Tham, A. K. Sen, A. Sekiguchi, R. G. Greaves, and G. A. Navratil, Phys. Rev. Lett. **67**, 204 (1991).
[18] B. Richards, T. Uckan, A. J. Wootton, B. A. Carreras, R. D. Bengtson, P. Hurwitz, G. X. Li, H. Lin, W. L. Rowan, H. Y. W. Tsui, A. K. Sen, and J. Uglum, Phys. Plasmas **1**, 1606 (1994).
[19] B. Richards, T. Uckan, A. J. Wootton, B. A. Carreras, R. D. Bengtson, D. Crockett, K. W. Gentle, P. Hurwitz, G. X. Li, H. Lin, W. L. Rowan, and H. Y. W. Tsui, Bull. Am. Phys. Soc. **37**, 1388 (1992).
[20] T. Uckan, B. Richards, R. D. Bengtson, B. A. Carreras, G. X. Li, P. D. Hurwitz, W. L. Rowan, H. Y. W. Tsui, and A. J. Wootton, Nucl. Fusion **35**, 487 (1995).
[21] T. Uckan, B. Richards, A. J. Wootton, R. D. Bengtson, R. Bravenec, B. A. Carreras, G. X. Li, P. Hurwitz, P. E. Phillips, W. L. Rowan, H. Y. W. Tsui, J. R. Uglum, Y. Wen, and D. Winslow, J. Nucl. Mater. **220-222**, 663 (1995).
[22] *Feedback and Dynamic Control of Plasmas*, edited by T. K. Chu and H. W. Hendel (AIP, New York, 1970).
[23] K. Zhai, Y. Z. Wen, C. X. Yu, W. D. Liu, C. Wang, G. Zhuang, and Z. Z. Xu (unpublished).
[24] D. E. Smith, E. J. Powers, and G. S. Caldwell, IEEE Tran. Plasma Sci. **2**, 261 (1974).
[25] E. J. Powers, Nucl. Fusion **14**, 749 (1974).
[26] J. M. Beall, Y. C. Kim, and E. J. Powers, J. Appl. Phys. **53**, 3933 (1982).
[27] S. J. Levinson, J. M. Beall, E. J. Powers, and R. D. Bengtson, Nucl. Fusion **24**, 527 (1984).
[28] Ch. P. Ritz, E. J. Powers, T. L. Rhodes, R. D. Bengtson, K. W. Gentle, H. Lin, P. E. Phillips, A. J. Wootton, D. L. Brower, N. C. Luhmann, Jr., W. A. Peeble, P. M. Schoch, and R. L. Hickok, Rev. Sci. Instrum. **59**, 1739 (1988).
[29] S. J. Zweben and R. J. Taylor, Nucl. Fusion **21**, 193 (1981).
[30] S. J. Zweben and R. W. Gould, Nucl. Fusion **25**, 171 (1985).
[31] S. L. Chen and T. Sekiguchi, J. Appl. Phys. **36**, 2363 (1965).
[32] Y. H. Xu, G. D. Wang, K. Zhai, C. Wang, W. D. Liu, and C. X. Yu, Phys. Plasma **3**, 1022 (1996).
[33] M. Kono and E. Miyashita, Phys. Fluids **31**, 326 (1988).
[34] A. Muhm, A. M. Pukhov, K. H. Spatschek, and V. Tsytovich, Phys. Fluids B **4**, 336 (1992).
[35] Y. C. Kim and E. J. Powers, Phys. Fluids **21**, 1452 (1978).
[36] Y. C. Kim and E. J. Powers, IEEE Tran. Plasma Sci. **7**, 120 (1979).